Clustering in randomly driven Hamiltonian systems

D. V. Makarov, M. Yu. Uleysky, M. V. Budyansky, and S. V. Prants
Laboratory of Nonlinear Dynamical Systems, V.I. Il'ichev Pacific Oceanological Institute of the Russian Academy of Sciences, 690041 Vladivostok, Russia

(Received 15 July 2005; revised manuscript received 21 April 2006; published 8 June 2006)

The motion of oscillatorylike nonlinear Hamiltonian systems, driven by a weak noise, is considered. A general method to find regions of stability in the phase space of a randomly driven system, based on a specific Poincaré map, is proposed and justified. Physical manifestations of these regions of stability are *coherent clusters*. We illustrate the method and demonstrate the appearance of coherent clusters with two models motivated by the problems of waveguide sound propagation and Lagrangian mixing of passive scalars in the ocean. We find bunches of sound rays propagating coherently in an underwater waveguide through a randomly fluctuating ocean at long distances. We find clusters of passive particles to be advected coherently for a comparatively long time by a random two-dimensional flow modeling mixing around a fixed vortex.

DOI: 10.1103/PhysRevE.73.066210 PACS number(s): 05.45.−a, 05.40.Ca, 92.10.Vz, 47.52.+j

I. INTRODUCTION

The interplay between dynamical chaos and noise is a topic of interest both in nonlinear dynamics and statistical physics. Real-world systems operate against a noisy background. Both chaos and noise mean random or diffusivelike behavior in the nonlinear system's dynamics that can be quantified by the maximal Lyapunov exponents,

$$\lambda = \lim_{t\to\infty} \lambda(t), \quad \lambda(t) = \lim_{\Delta(0)\to 0} \frac{1}{t} \ln \frac{\Delta(t)}{\Delta(0)}, \tag{1}$$

where $\Delta(t)$ is a distance (in the Euclidean sense) in a direction at the moment t between two initially closed trajectories.

However, the methods and approaches to study a deterministic and random system are different. Typical deterministic nonlinear systems (the so-called nonhyperbolic system) are known to have mixed phase space with coexisting regions of stable and unstable motion. There are islands of regular motion merged into a chaotic sea, islands around islands, stochastic layers confined between invariant tori, cantori near the boundaries of islands, and so on (for a recent review of chaos in Hamiltonian systems see [1]). The motion is predictable in some regions but permits a statistical description only in those where extremal sensitivity to initial conditions takes place. The notion of the mixing time, the reciprocal maximal Lyapunov exponent, can be introduced to quantify the so-called predictability horizon $\tau_p \approx \lambda^{-1} \ln(\delta x/\delta x_0)$, where δx is a confidence interval of a dynamical variable x and δx_0 is an inevitable unaccuracy in fixing its initial value.

To describe randomly driven systems one uses some ergodic postulates based on the assumption of fully developed chaos. In Hamiltonian nonintegrable systems, intermittentlike dynamics with chaotic oscillations interrupted by regular ones seems to be more realistic. It means, in particular, that regular motion does not cease suddenly, and completely stochastic motion does not arise suddenly just beyond the predictability horizon. Remnants of stability should persist for more long times. It is especially true for oscillatorylike systems due to resonant interaction of unperturbed motion with random perturbation [2].

In this paper we treat a model of a randomly driven nonlinear oscillator from a purely deterministic point of view, and show that there are regions of stability surviving for a comparatively long time under a weak noisy excitation with an arbitrary spectrum. This time can be estimated with the help of a specific map that plays the role of the Poincaré map in periodically driven systems. The map is intended to find numerical clusters of trajectories with close initial conditions which are stable by Lyapunov with a given realization of the random perturbation (Sec. II). We check the effectiveness of the procedure proposed with two models motivated by the problems of waveguide sound propagation and Lagrangian mixing of passive scalars in the ocean where, as in other geophysical problems, there is, as a rule, no respective statistical ensemble of averaging, and we deal with single realizations in the field experiments. Noise-induced coherent clusters are demonstrated with the ray model of sound propagation in an ocean waveguide with a randomly fluctuating sound-speed profile induced by internal waves in the deep ocean (Sec. III). Another example is clustering of passive particles advected by a random two-dimensional velocity field in an ideal fluid (Sec. IV).

II. EFFECTIVE POINCARÉ MAP

In this section we introduce an effective Poincaré map that, like to the usual Poincaré map, enables us to find numerically regions of stability in the phase space of a Hamiltonian system surviving under a weak random perturbation due to nonlinear resonances between the unperturbed motion and the perturbation.

Let us consider a one-dimensional nonlinear oscillator with the Hamiltonian

$$H = H_0 + \varepsilon H_1(t) = \frac{p^2}{2} + U(q) + \varepsilon V(q)\xi(t), \tag{2}$$

where q and p are position and momentum, $U(q)$ is an unperturbed potential, $V(q)$ is a smooth function, $\xi(t)$ is a weak noise with $\varepsilon \ll 1$, and normalized first and second moments, $\langle \xi \rangle = 0$ and $\langle \xi^2 \rangle = 1/2$. Hereafter, we will consider a single

realization of noise, $\xi(t)$, and, therefore, the equations of motion,

$$\frac{dq}{dt} = p, \quad \frac{dp}{dt} = -\frac{dU}{dq} - \varepsilon \frac{dV}{dq}\xi(t), \tag{3}$$

can be treated as deterministic ones. Introducing the canonical transformation from the (q,p) variables to the action-angle variables (see [1,3]),

$$I = \frac{1}{2\pi}\oint p\, dq, \quad \vartheta = \frac{\partial}{\partial I}\int_{q'}^{q} p(q,H)dq, \tag{4}$$

we rewrite Eqs. (3) in the form

$$\frac{dI}{dt} = -\frac{\partial H(I,\vartheta)}{\partial \vartheta} = -\varepsilon \frac{\partial V(I,\vartheta)}{\partial \vartheta}\xi(t),$$

$$\frac{d\vartheta}{dt} = \frac{\partial H(I,\vartheta)}{\partial I} = \omega(I) + \varepsilon \frac{\partial V(I,\vartheta)}{\partial I}\xi(t), \tag{5}$$

where $\omega(I) \equiv \partial H_0/\partial I$ is an action-dependent characteristic frequency of oscillations.

The notion of stability means a weak sensitivity of a solution to small changes in initial conditions that is quantified by the Lyapunov exponent (1). As we know from KAM theory [4], most of the invariant tori of integrable Hamiltonian systems, where the motion is stable, are preserved under a small perturbation. In spite of each single realization of a random perturbation, $\xi(t)$ can be treated more as a deterministic function than a stochastic one; an infinite number of frequencies in the spectrum of $\xi(t)$ leads to densely distributed resonances in the phase space and lacking of invariant tori. In the limit $t \to \infty$, no regions in the phase space remain forbidden under a noisy perturbation. Even a weak noise can accelerate phase-space transport by forcing trajectories to traverse KAM tori [3,5,6]. So a deterministic description ceases to have a sense, and one forces us to use a statistical description of the motion.

However, in practice, we deal with a finite time interval $[0:T_0]$. Moreover, in geophysical field experiments, the experimentalists work mainly with single realizations of nonstationary processes of interest. By these reasons we can recover "deterministic" methods to explore the sets of stable trajectories satisfying to the condition of the finite-time invariance: *if any set in the phase space at* $t=0$ *transforms to itself at* $t=T_0$ *without mixing, then it corresponds to an ensemble of trajectories that are stable by Lyapunov within the interval* $[0:T_0]$. In order to find such stable sets for an arbitrary spectrum of perturbation, we propose the following map:

$$I_{i+1} = I(t = T_0, I_i, \vartheta_i), \quad \vartheta_{i+1} = \vartheta(t = T_0, I_i, \vartheta_i). \tag{6}$$

We start at $t=0$ with initial conditions $I(0)=I_i$ and $\vartheta(0)=\vartheta_i$ and compute the solution of Eqs. (5), I_{i+1} and ϑ_{i+1}, at the moment $t=T_0$ with a given realization of a noise $\xi(t)$ over the interval $[0:T_0]$. Those values, I_{i+1} and ϑ_{i+1}, are chosen as new initial conditions for computing the next solution of Eqs. (5), I_{i+2} and ϑ_{i+2}, at the moment $t=T_0$ with the same realization of $\xi(t)$, and so on. In fact, this map is equivalent to a Poincaré map for a system with the Hamiltonian,

$$H = H_0(I) + \varepsilon V(I,\vartheta)\tilde{\xi}(t), \tag{7}$$

where $\tilde{\xi}(t)$ is a periodic function consisting of identical pieces of $\xi(t)$ of the same duration T_0,

$$\tilde{\xi}(t + nT_0) = \xi(t), \quad 0 \le t \le T_0, \quad n = 0,1,\ldots . \tag{8}$$

In this way we replace our original randomly driven system by a periodically driven one. It should be emphasized that the validity of this replacement is restricted by the time interval $[0:T_0]$. By analogy with the usual Poincaré map, the key property of the map (6) is the following: *each point of a continuous closed trajectory of the map* (6) *corresponds to a starting point of the solution of Eqs.* (5)*, which remains stable by Lyapunov until the time* T_0. The inverse statement is not, in general, true. It will be shown later that the map (6) provides sufficient but not necessary the criterion of stability. Topological properties of trajectories of the map (6) can be treated in the framework of the theory of nonlinear resonance [5]. The functions $V(I,\ \vartheta)$ and $\tilde{\xi}(t)$ can be decomposed in a Fourier series;

$$V(I,\vartheta) = \sum_{l=-\infty}^{\infty} V_l(I)\exp[i(l\vartheta + \phi_l)],$$

$$\tilde{\xi}(t) = \sum_{m=-\infty}^{\infty} \xi_m \exp[i(m\Omega t + \psi_m)], \tag{9}$$

where $\Omega = 2\pi/T_0$. The Fourier amplitudes of the analytic function V decay as $V_l(I) \sim \exp(-\sigma l)$, whereas the ones for the random function $\xi(t)$ decay as $\xi_m \sim m^{-\beta}$ ($0 \le \beta \le 1$ and $\beta = 0$ for a white noise), since $\xi(0) \ne \xi(T_0)$. If the interval T_0 is large enough, the parameter β is determined mainly by the correlation time of $\xi(t)$.

Substituting the expansions (9) into the equations of motion (5) and omitting rapidly oscillating terms $\exp[i(l\vartheta + m\Omega t)]$, we get the following equations:

$$\frac{dI}{dt} = -\frac{i\varepsilon}{2}\sum_{l,m=0}^{\infty} lV_l\xi_m \exp i\Phi + \text{c . c .},$$

$$\frac{d\vartheta}{dt} = \omega + \frac{\varepsilon}{2}\sum_{l,m=0}^{\infty} \frac{\partial V_l}{\partial I}\xi_m \exp i\Phi + \text{c . c .}, \tag{10}$$

where $\Phi = l\vartheta - m\Omega t + \phi_l - \psi_m$. The stationary phase condition $d\Phi/dt = 0$ implies the resonances of the map (6),

$$mT(I) = lT_0, \tag{11}$$

where $T(I) = 2\pi/\omega(I)$ is a period of unperturbed oscillations with a given value of the action I. Resonant values of the action I_{res} can be found from the condition (11). The relation $l:m$ defines the order of the respective resonance. It should be noted that an infinite number of resonances $jl:jm$ ($j = 1,2,\ldots$) corresponds simultaneously to each value of the resonant action. However, if I_{res} is far enough from the sepa-

ratrix value, the product $V_l\xi_m$ decreases rapidly with increasing j, and the resonances with small values of l and m only can affect significantly a trajectory. Thus, if $T_0 > T(I_{\rm res})$, only the superior term with $l=1$ should be taken into account. Neglecting the higher-order resonances, we can describe the motion in the vicinity of $I_{\rm res}$ in the pendulum approximation [5]. Leaving the resonant term only, we can rewrite Eqs. (10) in the form

$$\frac{dI}{dt} = \varepsilon V_1(I_{\rm res})\xi_m \sin\Phi,$$

$$\frac{d\Phi}{dt} = \omega - m\Omega + \varepsilon \frac{\partial V_1(I_{\rm res})}{\partial I}\xi_m \cos\Phi, \tag{12}$$

which corresponds with some simplification to the universal Hamiltonian of nonlinear resonance [1,5],

$$H_u = \frac{1}{2}|\omega_I'|(\Delta I)^2 + \varepsilon V_l \xi_m \cos\Phi, \tag{13}$$

where $\Delta I = I - I_{\rm res}$. Solutions of Eqs. (12) describe oscillations of the action I and phase Φ variables near elliptic fixed points of the respective resonances, the so-called phase oscillations.

An angular location of the fixed points depends on a random phase ψ_m and, therefore, varies from one realization of the random function $\xi(t)$ to another. A trajectory of the map (6), being captured into a resonance, draws a chainlike structure in the phase space. In the regime of stable motion, neighboring chains are far enough from each other, and the space between them is filled by nonresonant stable trajectories. The width of the resonance in terms of the frequency can be estimated from the Hamiltonian (13) as follows:

$$\Delta\omega = |\omega_I'|\Delta I_{\max} \simeq 2\sqrt{\varepsilon|\omega_I'|V_1\xi_m}, \tag{14}$$

where $\omega_I' = d\omega/dI$ is related to nonlinearity of oscillations and determined by the form of the unperturbed potential. The distance between the neighboring resonances of the successive orders is $\delta\omega(T_0) = 2\pi/T_0$. If the criterion of Chirikov, $\Delta\omega/\delta\omega \simeq 1$, holds, the resonances overlap in the phase space, the phase oscillations become unstable, and global chaos emerges.

The time $T_{\rm c}$, required for overlapping all the resonances in the phase space, is determined from the specific Chirikov's relation,

$$\frac{\Delta\omega(I_{\min})}{\delta\omega(T_c)} = 1, \tag{15}$$

where $\Delta\omega(I_{\min})$ is a width of the deepest resonance. If the Chirikov's criterion (15) is satisfied with the deepest resonance, i.e., for the resonance with the minimal value of the action $I_{\min}$, the stochastic sea covers all the accessible phase space. The respective time $T_{\rm c}$ can be estimated directly from Eq. (15) to be

$$T_{\rm c} \simeq \frac{\pi}{\sqrt{\varepsilon|\omega_I'|V_1(I_{\min})\xi_m}}, \tag{16}$$

where the amplitudes ξ_m are supposed to be independent of time. It may be treated as a lower limit of time when mixing affects all the accessible phase space. Nevertheless, some stable regions in the phase space, satisfying the condition of the finite-time invariance, can survive at $T > T_{\rm c}$ in the form of islands submerged into a stochastic sea. There may exist weakly chaotic orbits with small maximal Lyapunov exponents $\lambda < 1/T_c$ that can behave like stable noisy orbits at $t > T_c$. However, they do not belong to the sets satisfying the condition of the finite-time invariance (except for a zero measure set), and the map (6) does not "see" such trajectories. With a given spectrum of noise and large enough values of T_0, the difference between the amplitudes ξ_m for different realizations of the noise becomes negligible. Therefore, the time of phase correlations $T_{\rm c}$ is independent of the realization chosen and may be treated as a characteristic quantity of a Hamiltonian system under consideration.

III. CLUSTERING OF SOUND RAYS IN AN OCEAN WAVEGUIDE

Low-frequency acoustic signals may propagate in the deep ocean to very long ranges due to the existence of the underwater sound channel, which acts as a waveguide confining sound waves within a restricted water volume (see the general theory in Ref. [7] and a description of the field experiments in the Pacific ocean in the issue [8]). In the geometric optics approximation, the underwater sound ray trajectories in a two-dimensional waveguide in the deep ocean with the sound speed c, being a smooth function of depth z and range r, satisfy the canonical Hamiltonian equations

$$\frac{dz}{dr} = \frac{\partial H}{\partial p}, \quad \frac{dp}{dr} = -\frac{\partial H}{\partial z}, \tag{17}$$

with the Hamiltonian

$$H = -\sqrt{n^2(z,r) - p^2}, \tag{18}$$

where $n(z,r) = c_0/c(z,r)$ is the refractive index, c_0 is a reference sound speed, $p = n\sin\phi$ is the analog to mechanical momentum, and ϕ is a ray grazing angle. In the paraxial approximation (that takes into account rays launched at comparatively small grazing angles that can propagate in the ocean at a long distance without touching the lossy bottom), the Hamiltonian can be written in a simple form as a sum of the range-independent and range-dependent parts,

$$H = H_0 + H_1(r), \tag{19}$$

with

$$H_0 = -1 + \frac{p^2}{2} + \frac{\Delta c(z)}{c_0}, \quad H_1(r) = \frac{\delta c(z,r)}{c_0}, \tag{20}$$

where $\Delta c(z) = c(z) - c_0$ describes variations of the sound speed along the waveguide and $p \simeq \tan\phi$. The term H_1 describes variations of the sound speed caused, mainly, by internal waves in the ocean.

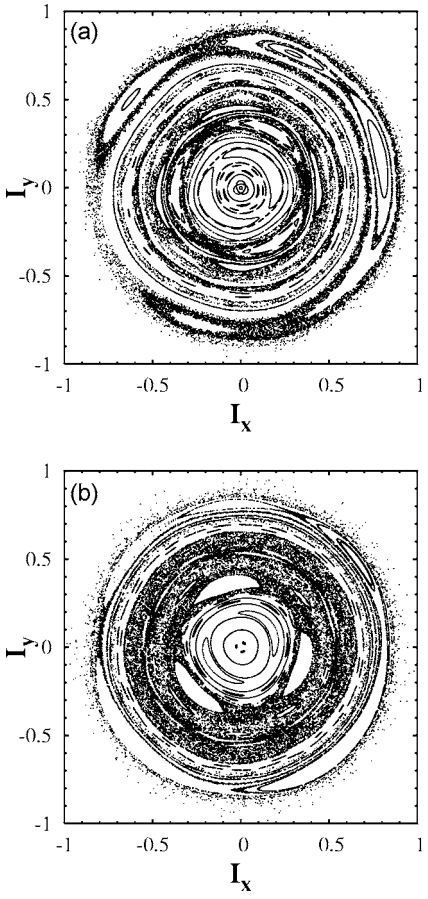

FIG. 1. The map (24) with $d=100$ km revealing stable bundles of sound rays surviving in a model underwater waveguide under a noisy-like internal-wave perturbation (23) with a single vertical mode (29). The polar action-angle variables $I_x=(I/I_s)\cos\theta$ and $I_y=(I/I_s)\sin\theta$ are in units of the separatrix action I_s. Fragments (a) and (b) correspond to two different realizations of noise at the same other conditions.

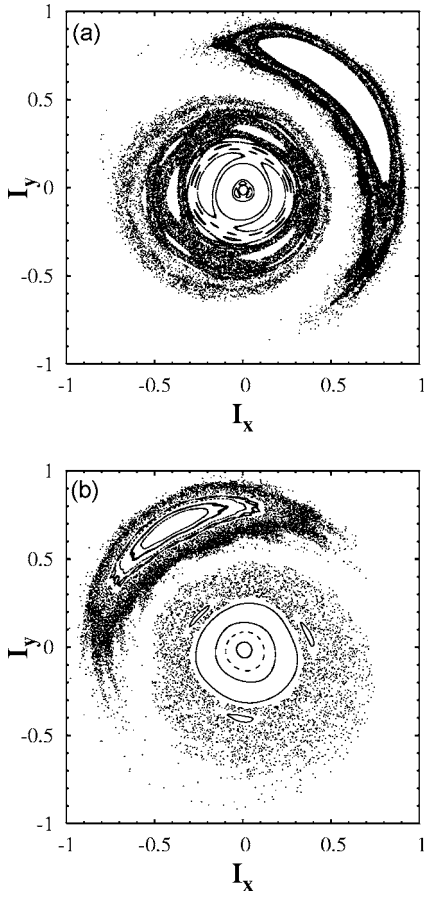

FIG. 2. The same as in Fig. 1 but with five vertical modes (30), $d=100$ km. Fragments (a) and (b) correspond to two different realizations of noise at the same other conditions.

In a simplified model of perturbation with δc being a periodic function of the range r, the extremal sensitivity of ray trajectories to initial conditions—ray dynamical chaos—has been found [9,10]. More realistic models should include not only horizontal but vertical modes of internal waves as well. Moreover, the internal waves perturbation is stochastic in the real ocean. In a number of recent publications [2,11–13], it has been realized that ray chaos should play an important role in interpretating the long-range field experiments [8,14,15]. In those experiments groups of rays with close times of arrivals to a fixed range have been found in the early arriving parts of the sound signals. In Refs. [16–19] such rays with the same number of the turning points along the propagation paths were called "clusters." It should be noted that rays belonging to such a cluster may propagate along rather different paths and even be chaotic.

We use a background sound-speed profile introduced in Ref. [20] to model sound propagation through the deep ocean,

$$c(z) = c_0\left(1 - \frac{b^2}{2}(\mu - e^{-az})(e^{-az} - \gamma)\right), \quad 0 \le z \le h, \tag{21}$$

where $\gamma=e^{-ah}$, μ, a, and b are adjusting parameters, h is the maximal depth, and $c_0=c(h)$. We represent the perturbation of the background sound-speed profile along the waveguide in the following form:

$$\frac{\delta c(z,r)}{c_0} = \varepsilon V(z)\xi(z,r), \tag{22}$$

where $\varepsilon \ll 1$, $V(z)$ describes sound-speed fluctuations along the vertical coordinate z, and $\xi(z,r)$ is a fluctuation field with $\langle\xi\rangle=0$ and $\langle\xi^2\rangle=1/2$. Let us assume that the stochastic perturbation can be written in the factorized form

$$\xi(z,r) = X(z)Y(r). \tag{23}$$

Our aim is to find the bundles of sound rays that are stable up to a distance d from a source. After making the canonical transformation from a ray variables (z,p) to the action-angle ones (I,ϑ), we use the effective Poincaré map (6), which now takes the form

$$I_{i+1} = I(d; I_i, \vartheta_i),$$

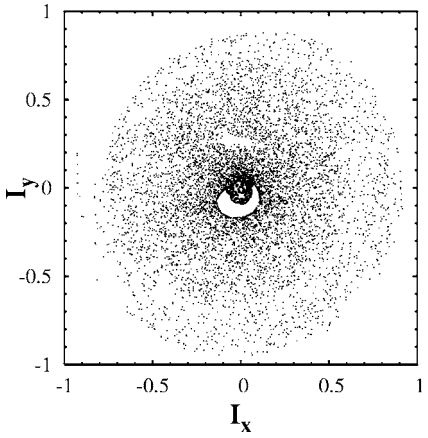

FIG. 3. The same as in Fig. 2, but with $d=500$ km.

$$\vartheta_{i+1} = \vartheta(d; I_i, \vartheta_i). \tag{24}$$

Let us expand $Y(r)$ in the Fourier series,

$$Y(r) = \frac{1}{2}\sum_{m=-\infty}^{\infty} Y_m e^{imk_r r}, \tag{25}$$

where $k_r = 2\pi/d$, and represent $X(z)$ as a sum of vertical modes,

$$X(z) = \frac{1}{2}\sum_{n=-\infty}^{\infty} X_n e^{in\pi\chi(z)}, \tag{26}$$

where $\chi(z) = e^{-z/B} - e^{-h/B}$, and B is a thermocline depth. Substituting (25) and (26) into the equations of motion,

$$\frac{dI}{dr} = -\frac{1}{c_0}\frac{\partial(\delta c)}{\partial\vartheta}, \quad \frac{d\vartheta}{dr} = \omega + \frac{1}{c_0}\frac{\partial(\delta c)}{\partial I}, \tag{27}$$

and using the condition of the stationary phase, one gets the resonance conditions in the form that demonstrates explicitly the role of a resonance with the vertical oscillations of the internal waves [see the third terms in Eqs. (28)],

$$l\omega - mk_r \pm n\pi p\frac{e^{-z/B}}{B} = 0,$$

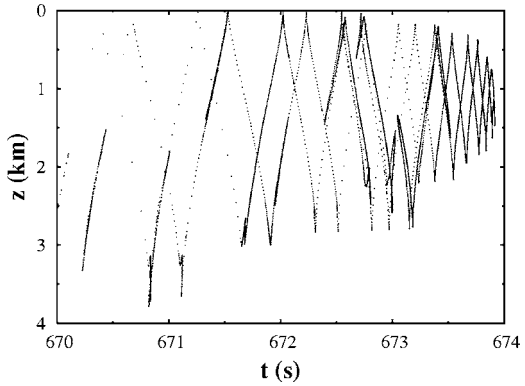

FIG. 4. Time front at the range 1000 km under the stochastic perturbation (25) and (30): ray depth z versus ray travel time t. Strips indicate coherent ray clusters.

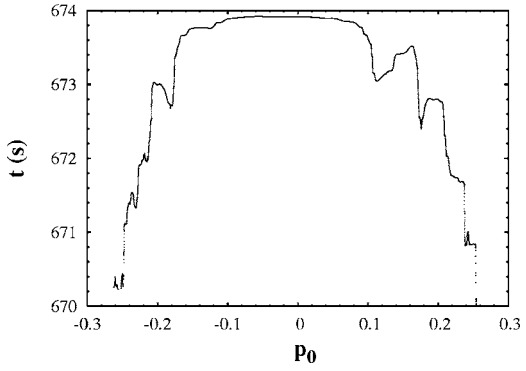

FIG. 5. Ray travel time t at the range 1000 km versus starting momentum p_0, which is a tangent of the initial grazing angle. Shelves indicate coherent ray clusters.

$$l\omega + mk_r \pm n\pi p\frac{e^{-z/B}}{B} = 0, \tag{28}$$

where l, m, and n take non-negative values only.

As it is seen from (28), vertical oscillations of the speed of sound give an additional term in the resonance conditions proportional to p and produce a special type of nonlinear resonances that can break regions of stability in the phase space. So the question is as follows: could those stable bundles of sound rays survive under a combined horizontal and vertical stochastic perturbation? The horizontal perturbation $Y(r)$ is modeled as a sum of a large (of the order of 1000) number of harmonics with random phases and the wave numbers distributed in the range from $k_{\min} = 2\pi/100$ km^{-1} to $k_{\max} = 2\pi$ km^{-1}. The spectral density of the perturbation decays as k^{-2}.

Let the vertical oscillations contain a single mode only,

$$X(z) = X_1 \sin \pi\chi(z), \tag{29}$$

and the other parameters are as follows: $\varepsilon = 0.0025$, $V(z) = (2z/B)e^{-2z/B}$, and $B = 1$ km. We start with a number of initial values of the ray action-angle variables in different regions of the phase space (I_0, θ_0) and compute their values at

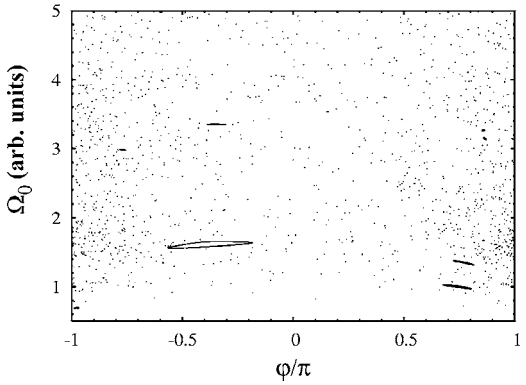

FIG. 6. The map (6) with $T_0 = 6\pi$ revealing regions of stability in a random velocity field with the amplitude $\varepsilon = 0.01$ and the frequency band $\omega \in [2:5]$. The unperturbed frequency of rotation of particles around the point vortex Ω_0 is in arbitrary units and the polar angle φ is in units of π.

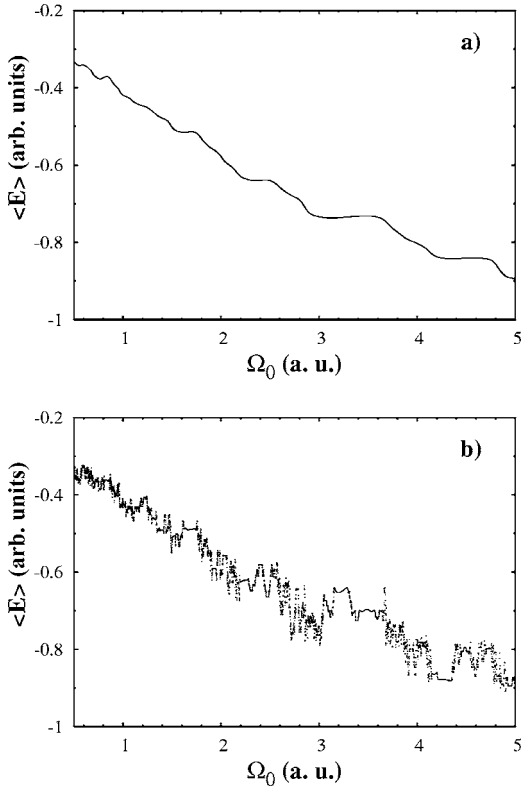

FIG. 7. The averaged (over T_0) "energy" of particles $\langle E \rangle$ versus their unperturbed frequency Ω_0: (a) $T_0=6\pi$ and (b) $T_0=30\pi$. Shelves indicate clusters of particles. Parameters of noise are given in the caption of Fig. 6.

the distance $d=100$ km (I_1, θ_1) from a sound source with the respective equations of ray motion with a chosen realization of the noisylike horizontal internal-wave perturbation (22) and the single vertical mode (29). Then we compute the ray variables with the same realization of noise at the same distance $d=100$ km, find (I_2, θ_2), and so on. The results of computing of the Poincaré map with two different realizations of noise in the coordinates $I_x=(I/I_s)\cos\vartheta$ and $I_y=(I/I_s)\sin\vartheta$ with $I_s=I(H=-1)$, being the separatrix value of the action, are shown in Fig. 1. Analytical expressions for the action I and angle ϑ variables in terms of the position z and momentum p variables are complicated functions that have been derived in an explicit way for the range-independent profile (21) in Sec. 3B in Ref. [2].

The map reveals numerous islandlike regions of stability in the phase space corresponding to the resonance condition $mD(I) \simeq ld$, where $D(I)$ is a cycle length of a ray with a given action I. The values of the island's areas and of the respective action are close with different realizations, but the island's form and their angle coordinates may be different.

Let us consider now a more complicated model with five vertical modes of internal waves,

$$X(z) = \sum_{n=1}^{5} X_n \sin[n\pi\chi(z) + \phi_n], \tag{30}$$

where $X_n \propto n^{-2}$, and ϕ_n are random phases. As it was shown in Ref. [19], this perturbation describes adequately sound propagation in a realistic ocean environment at low acoustic frequencies. The respective maps (24) are shown in Fig. 2 with $d=100$ km and with two different realizations of noise. It follows from comparing Figs. 1 and 2 that the complication in the vertical perturbation effects, mainly, the most steep rays corresponding to the outer resonance islands. The most outer islands in Fig. 2 are separated from the other domains of stability by a layer of escaping rays (by escaping rays we mean the rays quitting by different reasons the sound waveguide during their propagation). Comparing Figs. 2(a) and 2(b), we see that under different realizations of noise the outer region of stability is of approximately the same area and topology and changes its angular position only. With increasing d, the area of islands decreases but distinct islands of stability remain visible in the phase space at a rather long distance $d=500$ km (Fig. 3), even with five vertical modes of internal waves to be included in the model.

The practical question is as follows: in which way are the regions of stability manifested in real field experiments? What is measured in the field experiments is the time of arrivals of sound signals and the depths of their arrivals at a given range R with the help of a vertical receiving array of hydrophones [8,14,15]. We compute the so-called timefront at $R=1000$ km, solving not the map (24) but the equations of motion (17) with the stochastic perturbation (25) and (30). The prominent almost vertical strips in Fig. 4 belong to those rays that propagate coherently and arrive at the fixed range 1000 km at practically the same time. Such rays belong to *coherent clusters*. The rays in a coherent cluster do arrive at the fixed range at closed times and move coherently when propagating through the fluctuating ocean different from the clusters to be described in Refs. [18,16,17,19]. It should be emphasized that similar strips have been found in the field experiments [8,14,15,21].

In conclusion of this section, we show manifestations of coherent ray clusters in the so-called $t-p_0$ plot. Figure 5 demonstrates the ray travel time t as a function of the starting ray momentum p_0 at the distance $R=1000$ km from a sound source for the model with a purely horizontal random perturbation, i.e., Eq. (23) with $X(z)=1$. The main feature of this dependence is "shelves," i.e., more or less flat segments in the $t-p_0$ plot. Each "shelf" corresponds to a coherent cluster. The "shelves" are distributed chaotically over the range of the starting momenta, and their positions depend on a specific realization of the random perturbation. Such "shelves" have been found with different kinds and realizations of the internal-wave induced random perturbation, proving that the appearance of coherent clusters is a common feature in the sound-waveguide propagation through a fluctuating ocean. It should be noted that in the case of periodically perturbed waveguides similar "shelves" have been first found numerically in Ref. [22] and explained to be caused by nonlinear resonances of rays with the periodic perturbation.

In underwater acoustics measuring and computing $z-t$ and $t-p_0$ plots give us a rear possibility to fix coherent clusters directly. There is a close connection between the coherent clusters and the regions of stability in the phase space to be revealed with the help of the map (24). Rays, forming a coherent cluster, propagate near the regions of stability. That is why they do not diverge in the stochastic environment. In

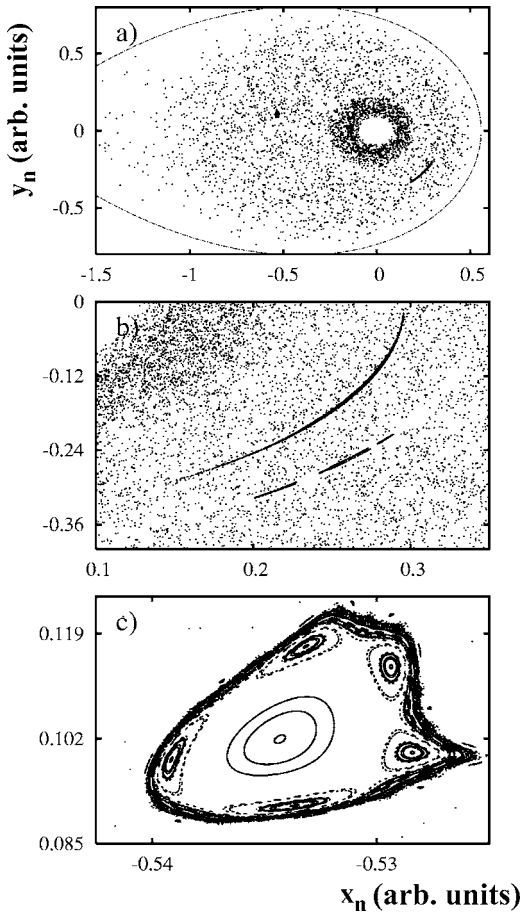

FIG. 8. The map (6) with $T_0=2.3\pi$ revealing regions of stability in a random velocity field with the amplitude $\varepsilon=0.1$ and the frequency band $\omega \in [9:10]$. (a) General view in the phase plane (x,y); (b) and (c) magnifications of the respective regions in (a). The dotted line is an unperturbed separatrix.

conclusion of this section, we would like to stress that the map (24) with a fixed value of d reveals only a part of the respective regions of stability, whereas time fronts and $t-p_0$ plots contain much more extensive regions of stability corresponding to coherent clusters (compare Fig. 3 with Figs. 4 and 5).

IV. CLUSTERING OF PASSIVE PARTICLES IN A TWO-DIMENSIONAL FLOW

In this section we consider clustering in a simple two-dimensional flow of an ideal fluid with the dimensionless streamfunction,

$$\Psi = \ln\sqrt{x^2+y^2} + \mu x + \varepsilon x\, \xi(\tau), \tag{31}$$

whose simplified version with $\xi(\tau)$ being a harmonic function has been introduced in Ref. [23] to the model advection of passive particles in a flow with a fixed point vortex [the first term in (31)], a stationary current along the axis y with the normalized velocity μ (the second term), and a harmonically alternating current with the normalized velocity ε. This simple model is motivated by the problem of Lagrangian mixing and transport of passive scalars in the flow around a topographical eddy over a seamount in the ocean randomly perturbed by wind in the surface layer or by small-scale turbulence. It is well known that the Hamiltonian equations of motion for particles (tracers) with Cartesian coordinates x and y in an incompressible two-dimensional flow are written as

$$\dot{x} = -\frac{\partial \Psi}{\partial y} = -\frac{y}{x^2+y^2},$$

$$\dot{y} = \frac{\partial \Psi}{\partial x} = \frac{x}{x^2+y^2} + \mu + \varepsilon\, \xi(\tau). \tag{32}$$

The configuration space of advection particles is the phase space of dynamical system (31), and it is possible to see noisy-induced clusters of particles in the flow (31) by a naked eye. We model the noise as a random function $\xi(\tau)$ consisting of a large number of harmonics,

$$\xi(\tau) = \frac{1}{\sqrt{N+1}} \sum_{n=0}^{N} \sin(\omega_n \tau + \varphi_n), \tag{33}$$

with random phases φ_n, and the frequencies

$$\omega_n = \omega_b + n\frac{\omega_e - \omega_b}{N}, \quad n = 0,1,\ldots,N, \tag{34}$$

distributed equally in the range $[\omega_b:\omega_e]$ between the lowest (ω_b) and highest (ω_e) frequencies. It is possible, in principle, to model the spectrum of an arbitrary form with the help of the series (33) introducing an amplitude factor depending on the frequency. According to the central limit theorem, $\xi(\tau)$ has a Gaussian distribution with a zero expectation value because it is a large number of independent random variables. The factor $1/\sqrt{N+1}$ provides the variance to be equal to $1/2$.

It is well known [24–26] that the advection of passive particles in periodic two-dimensional flows of ideal fluids may be chaotic in the sense of exponential sensitivity of the particle's motion to small variations in initial conditions. The advection of passive particles under a single-mode perturbation in the model (31) without any noise has been considered in detail in Refs. [27,28] as a scattering problem: particles enter a mixing zone around the vortex with the incoming current and escape from it with an outcoming flow. The scattering has been shown to be chaotic in the sense that there is a nonattracting invariant set, consisting of unstable periodic, aperiodic, and marginally unstable orbits, that determines scattering and trapping of particles from the incoming flow. The scattering has been shown to be fractal in the sense that scattering functions (namely, the dependence of the trapping time for particles and of the number of times they wind around the vortex on the initial particle's coordinates) are singular on a Cantor-like set of initial positions.

Now we are interested in what happens if that deterministic flow is perturbed by a weak noise. It should be noted, first of all, that fractality in the scattering functions does not disappear under noisy excitation, but the respective fractals have been shown to have a more complicated hierarchical

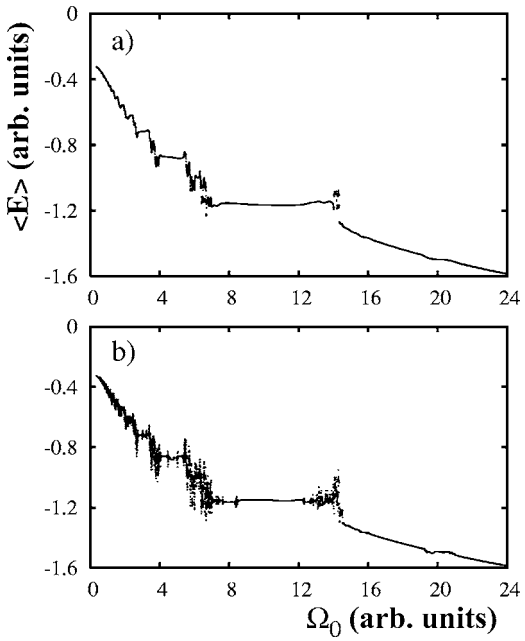

FIG. 9. The averaged (over T_0) "energy" $\langle E\rangle$ of particles versus their unperturbed frequency Ω_0: (a) $T_0=2.3\pi$ and (b) $T_0=10\pi$. Shelves indicate clusters of particles. Parameters of noise are given in the caption to Fig. 8.

structure. In order to find noisy-induced regions of stability, we use the effective Poincaré map of the type of (6) with different values of the time interval T_0, the amplitude of noise ε, and the frequency range of noise $[\omega_b:\omega_e]$.

In Fig. 6 we demonstrate the results of mapping (6) with $T_0=6\pi$ in the plane of the frequency Ω_0 of the rotation of particles around the vortex in the unperturbed system with $\varepsilon=0$ and the polar angle with $\tan\varphi=y/x$. A large number of particles advected by the flow (31) with $\mu=0.5$ and a chosen realization of the weak noise with the amplitude $\varepsilon=0.01$ and the medium-frequency range $\omega\in[2:5]$ has been chosen for simulation. The numerical experiments have been carried out with different random choices of phases in the series (33), i.e., with different realizations of noise. Regions of stable motion in the space have been observed with all the realizations in the form of islandlike structures with approximately the same values of their area and radial position.

In order to find manifestations of coherent clusters of passive particles, advected by the noisy flow, we compute the dependence of the stationary part of the streamfunction (31) averaged over T_0—the averaged "energy" $\langle E\rangle$—on their unperturbed frequency Ω_0 at initial positions. Due to a resonant interaction between some harmonics of noise and the first harmonics of the unperturbed motion [2], the streamfunctions of resonant particles oscillate around specific values during their motion. The oscillations resemble the phase oscillations at a nonlinear resonance in Hamiltonian systems with a periodic perturbation. The long-time stability of oscillations of streamfunctions (if any) results in equality of the respective values $\langle E\rangle$ along neighboring trajectories and, therefore, in forming horizontal shelves in the $\langle E\rangle(\Omega_0)$ dependence [see Figs. 7 and 9 (later)]. The shelves are smooth even when averaging over a long time T_0, and it means lacking an extremal sensitivity of particles, forming a coherent cluster, to small variations in initial conditions. With an increase of the interval of mapping T_0, noisy-induced clusters are reduced, of course, in their size, but even with $T_0=30\pi$, which is larger than the average period of perturbation almost by two orders of magnitude, the prominent shelves corresponding to small-size clusters are still seen in Fig. 7(b). The sizes of the clusters that can be estimated by the length of the corresponding shelves are much larger than the areas of the respective zones of stability to be revealed with the help of the map (6) because the map cannot reveal the whole region of stability. Moreover, the coherent clusters consist of not only stable particles but weakly chaotic ones as well.

In order to test the ability of the map (6) for "catching" the regions of stability with a stronger and high-frequency noise, we have carried out a series of numerical experiments with $\mu=0.5$ and the noise of the amplitude $\varepsilon=0.1$ and the high-frequency range $\omega\in[9:10]$. Figure 8(a) demonstrates the result of mapping with $T_0=2.3\pi$ on the configuration

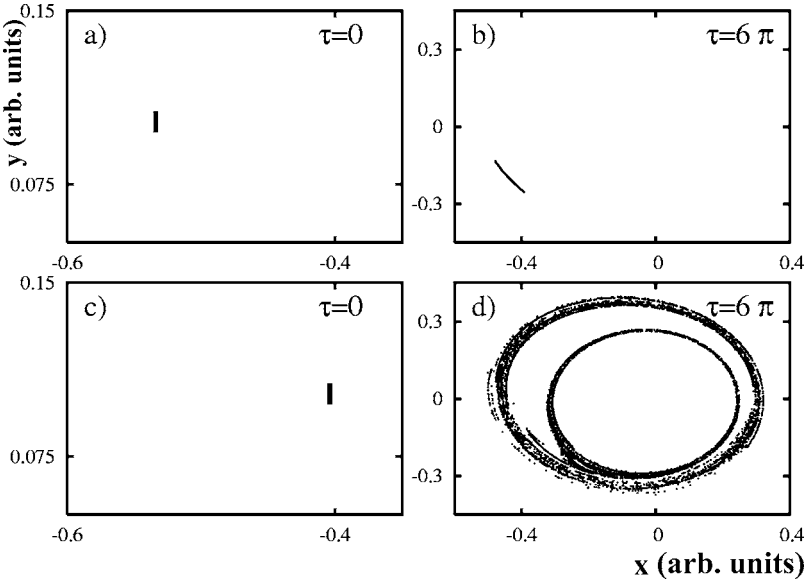

FIG. 10. The compact evolution of a coherent cluster of particles (the upper panel) and deformation of an unstable patch of particles (the lower panel) in a random velocity field. Parameters of noise are given in the caption to Fig. 8.

plane (x,y), and Figs. 8(b) and 8(c) are magnifications of the respective clusters in Fig. 8(a). Prominent chains of the islands of stability can survive under a rather strong noisy perturbation for a comparatively long time. Figure 9 demonstrates shelflike manifestations of noisy-induced clusters with $T_0=2.3\pi$ and $T_0=10\pi$.

To give a more direct manifestation of coherent clustering in a random flow that could be observed in real laboratory experiments with dye, we compare the evolution of patches of particles chosen in the regions of stability and instability in the configuration space. In the upper panel of Fig. 10, we show the evolution of a coherent cluster corresponding to the small black point (the region of stability for a given realization of noise) with coordinates $x\simeq -0.55$ and $y\simeq 0.1$ in Fig. 8(a). A more or less compact evolution of this patch with 10^4 particles goes on up to, at least, $\tau=6\pi$. For comparison, the lower panel of Fig. 10 demonstrates on the same time interval the evolution of the patch with the same number of particles chosen initially close to the coherent cluster at $\tau=0$. The respective initial patch is deformed strongly at $\tau=6\pi$ [29].

V. CONCLUSION

We proposed and justified a rather general method to find regions of stability in the phase space of oscillatorylike Hamiltonian systems driven by a weak noise with an arbitrary spectrum. Physical manifestations of these regions of stability, the so-called coherent clusters, have been demonstrated with two models. We have found coherent ray clusters in the model of underwater-waveguide sound propagation through a randomly fluctuating ocean and coherent clusters of passive particles in the two-dimensional flow modeling advection around a fixed vortex.

In conclusion, we would like to add two remarks about the properties of the effective Poincaré map (6). First, the temporal interval T_0 in constructing the map can be chosen arbitrarily along the time axis. Thus, if $\xi(t)$ is a stationary random process, the regions of stability in the phase space exist at any time moment. Second, the map (6) enables us to prove definitely the existence of some regions of stability, but not all of them. Really, the map, constructed with any given value of T_0, can reveal only those stable sets that correspond to the phase oscillations near the fixed points of the map. However, there exist another regions of stability looking as chaotic ones on the map. The topology of the map changes with varying the mapping time T_0, and some regions in the phase space, which look as pseudochaotic on the map at $T_0=T_1$, become stable at $T_0=T_2>T_1$. The total area of the regions of stability, survived under a weak noise at $t=T_0$, can be estimated as an area of superposition of all the stable sets detected by the map (6) with the mapping step varying from T_0 to T_c.

ACKNOWLEDGMENTS

This work was supported by the Russian Foundation for Basic Research (Project No. 06-05-96032), by the Program "Mathematical Methods in Nonlinear Dynamics" of the Prezidium of the Russian Academy of Sciences, and by the Program for Basic Research of the Far Eastern Division of the Russian Academy of Sciences.

[1] G. M. Zaslavsky, *Hamiltonian Chaos and Fractional Dynamics* (Oxford University Press, Oxford, 2005).
[2] D. V. Makarov, M. Yu. Uleysky, and S. V. Prants, Chaos **14**, 79 (2004).
[3] A. J. Lichtenberg and M. A. Lieberman, *Regular and Stochastic Motion* (Springer-Verlag, New York, 1983).
[4] V. I. Arnold, V. V. Kozlov, and A. I. Neishtadt, *Mathematical Aspects of Classical and Celestial Mechanics. Encyclopaedia of Mathematical Sciences* (Springer-Verlag, Berlin, 1988), Vol. 3.
[5] B. V. Chirikov, Phys. Rep. **52**, 265 (1979).
[6] A. B. Rechester, M. N. Rosenbluth, and R. B. White, Phys. Rev. A **23**, 2664 (1981).
[7] L. M. Brekhovskikh and Yu. Lysanov, *Fundamentals of Ocean Acoustics* (Springer-Verlag, Berlin, 1991).
[8] Special issue of J. Acoust. Soc. Am. **117**, 1499 (2005).
[9] S. S. Abdullaev and G. M. Zaslavsky, Zh. Eksp. Teor. Fiz. **80**, 524 (1981) [Sov. Phys. JETP **53**, 265 (1981)].
[10] S. S. Abdullaev and G. M. Zaslavsky, Usp. Fiz. Nauk **161**, 1 (1991) [Sov. Phys. Usp. **34**, 645 (1991)].
[11] J. Simmen, S. M. Flatté, and Guang-Yu Wang, J. Acoust. Soc. Am. **102**, 239 (1997).
[12] M. G. Brown, J. A. Colosi, S. Tomsovic, A. L. Virovlyansky, M. A. Wolfson, and G. M. Zaslavsky, J. Acoust. Soc. Am. **113**, 2533 (2003).
[13] M. A. Wolfson and S. Tomsovic, J. Acoust. Soc. Am. **109**, 2693 (2001).
[14] T. F. Duda, S. M. Flatté, J. A. Colosi, B. D. Cornuelle, J. A. Hildebrand, W. S. Hodgkiss, P. F. Worcester, B. M. Howe, J. A. Mercer, and R. C. Spindel, J. Acoust. Soc. Am. **92**, 939 (1992).
[15] P. F. Worcester, B. D. Cornuelle, M. A. Dzieciuch, W. H. Munk, B. M. Howe, J. A. Mercer, R. C. Spindel, J. A. Colosi, K. Metzger, T. J. Birdsall, and A. B. Baggeroer, J. Acoust. Soc. Am. **105**, 3185 (1999).
[16] F. D. Tappert and X. Tang, J. Acoust. Soc. Am. **99**, 185 (1996).
[17] I. P. Smirnov, A. L. Virovlyansky, and G. M. Zaslavsky, Chaos **12**, 617 (2002).
[18] A. L. Virovlyansky, J. Acoust. Soc. Am. **113**, 2523 (2003).
[19] K. C. Hegewisch, N. R. Cerruti, and S. Tomsovic, J. Acoust. Soc. Am. **117**, 1582 (2005).
[20] D. V. Makarov, M. Yu. Uleysky, and S. V. Prants, Pis'ma Zh. Tekh. Fiz. **29**, 70 (2003) [Tech. Phys. Lett. **29**, 430 (2003)].
[21] K. E. Wage, M. A. Dzieciuch, P. F. Worcester, B. H. Howe, and J. A. Mercer, J. Acoust. Soc. Am. **117**, 1565 (2005).
[22] S. S. Abdullaev and G. M. Zaslavsky, Sov. Phys. Acoust. **34**, 334 (1988).
[23] M. V. Budyansky and S. V. Prants, Pis'ma Zh. Tekh. Fiz. **27**,

51 (2001) [Tech. Phys. Lett. **27**, 508 (2001)].
[24] J. M. Ottino, *The Kinematics of Mixing: Stretching, Chaos, and Transport* (Cambridge University Press, Cambridge, 1989).
[25] S. Wiggins, Annu. Rev. Fluid Mech. **37**, 295 (2005).
[26] H. Aref, Phys. Fluids **14**, 1315 (2002).
[27] M. Budyansky, M. Uleysky, and S. Prants, Physica D **195**, 369 (2004).
[28] M. V. Budyansky, M. Yu. Uleysky, and S. V. Prants, Zh. Eksp. Teor. Fiz. **126**, 1167 (2004) [JETP **99**, 1018 (2004)].
[29] Animation available at: http://dynalab.poi.dvo.ru/papers/cluster.gif